

Ultrafast Chelation Dynamics of Cyclopentadienyl Manganese Tricarbonyl Derivatives with Pendant Sulfides

Jake S. Yeston,[†] Tung T. To,[‡] Theodore J. Burkey,^{*,‡} and Edwin J. Heilweil^{*,†}

Optical Technology Division, National Institute of Standards and Technology,
Gaithersburg, Maryland 20899-8443 and Department of Chemistry, Campus Box 526060,
University of Memphis, Memphis, Tennessee 38152-6060

Received: October 31, 2003; In Final Form: January 22, 2004

The photoinduced dynamics of two new $[\eta^5\text{-C}_5\text{H}_4\text{C}(\text{O})\text{R}]\text{Mn}(\text{CO})_3$ complexes **2** ($\text{R} = \text{CH}(\text{SCH}_3)_2$) and **3** ($\text{R} = \text{C}(\text{SCH}_3)_3$) have been investigated in *n*-heptane solution on the ps to μs time scale by UV-pump IR-probe transient absorption spectroscopy. Irradiation of **2** at 266 or 289 nm induces CO loss to yield two initial products in approximately equal abundance, assigned by their CO-stretching bands to be a heptane solvate of the unsaturated Mn fragment and a ring-formed product in which the pendant sulfide moiety is coordinated to the metal center. In direct analogy with the previously observed behavior of $[\eta^5\text{-C}_5\text{H}_4\text{C}(\text{O})\text{CH}_2(\text{SCH}_3)]\text{-Mn}(\text{CO})_3$ (**1**), the solvate reacts through a secondary pathway to afford the S-bound product within 200 ns. Irradiation of **3** under identical conditions yields the chelated product exclusively, with no evidence of a competing solvation pathway.

Introduction

We are investigating ring formation with organometallics as a mechanism for an ultrafast photoswitch. Cyclopentadienyl manganese tricarbonyl derivatives were selected because their UV photoinduced dynamics have been the subject of several studies and they have high yields for photosubstitution.^{1,2} In particular, the quantum yield is 0.65 for the photosubstitution of cyclopentadienyl manganese tricarbonyl with a free ligand. Like other metal carbonyls, we assumed that cage CO recombination reduces the quantum yield for substitution so we proposed that a pendant functional group might intercept the metal before CO recombination. Since CO recombination was found to be fast (<300 fs) relative to ring formation for small unstrained rings (~ 100 ps), we presumed that interception would only occur if the functional group was already near the metal upon CO dissociation.³

For the pendant sulfide **1** where the side chain conformations were not particularly restricted, we were surprised to find a unit quantum yield for chelation.⁴ We recently detailed the dynamics of the chelation reaction for complex **1** and found that chelation competes with solvation of the unsaturated metal center on the picosecond time scale, leading initially to a 1:1 ratio of solvated and ring-closed product (Scheme 1). The solvate is unstable and forms the chelation product within 70–100 ns, but this secondary pathway hampers the response time of chelation in its application as a photoswitch. We therefore prepared two new derivatives of the Mn species, **2** and **3**, bearing two and three pendant sulfide groups, respectively (Chart 1). The goal was to increase the probability for a sulfide group to be near the metal center, effectively accelerating the chelation and eliminating the competing solvation pathway. In this paper, we describe the photoinduced dynamics of **2** and **3** and compare them to our earlier results for **1**.

SCHEME 1

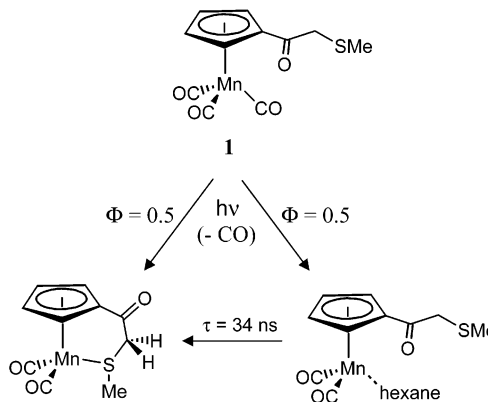
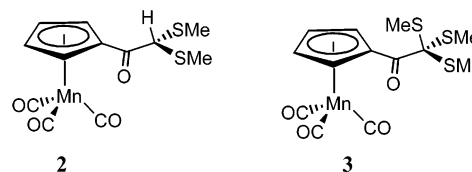


CHART 1



Experimental Section

A literature preparation of 2,2-bis(methylthio)-1-phenylethanone and 2,2,2-tris(methylthio)-1-phenylethanone from methyl benzoate and tris(methylthio)methyl lithium was modified to prepare **2** and **3**.⁵ A 2 M BuLi/hexane solution (13 mL, 26 mmol) was cannulated into a solution of tris(methylthio)methane (3.0 mL, 22.6 mmol) in 50 mL of THF at -95°C . Tricarbonyl-((carboxycyclopentadienyl)methyl ester) manganese (5.5 g, 25 mmol) in 20 mL of THF was likewise added. After 4 h of stirring, the solution was allowed to warm to room-temperature overnight. Upon quenching with water, extraction of the aqueous phase with ether, and evaporation of the organic phases, the

* To whom correspondence should be addressed. E-mail: edwin.heilweil@nist.gov; tburkey@memphis.edu.

[†] National Institute of Standards and Technology.

[‡] University of Memphis.

products were eluted with dichloromethane and hexane on silica gel, yielding 1.7 g of **2** (24%) and 2.9 g of **3** (36%).⁶

The transient absorption apparatus in our laboratory at NIST has been described in detail previously.⁴ Briefly, broadband IR generation is accomplished by difference frequency mixing in LiIO₃ between the visible output of two independently tunable synchronously pumped dye lasers (R6G, DCM), each of which is amplified at 20 Hz by the doubled output of a home-built Nd:YAG regenerative amplifier. We recently upgraded the CW Nd:YAG oscillator employed to pump the dye lasers and seed the amplifier. This diode-pumped passively mode-locked laser affords 2 W of 10 ps, 532 nm, extra-cavity doubled pulses at 80 MHz, as well as 1 W of 12 ps residual fundamental. Prior to seeding the amplifier, the fundamental pulses are temporally stretched by a factor of 10 to avoid damage to the amplifier cavity optics. Since the ps duration of these pulses renders traditional stretching methods inefficient, we employed a Littrow-blazed echelle grating to achieve a delay gradient along the horizontal dimension of the spatial beam profile. The grating is essentially used as a stair-shaped reflector, which is triple-passed for sufficient net delay across the beam. Spatial frequency dispersion from the grating is negligible in this case because the input pulses are narrowband.

The IR probe, once generated, is variably delayed using mirrors mounted on a computer-controlled translation stage. The beam is then split 1:1 to form a signal pulse, which overlaps with the UV pump in the sample, and a reference pulse, which probes an un-pumped region of the sample. Both signal and reference are dispersed in a monochromator and simultaneously detected using a liquid-nitrogen-cooled 256 × 256 element InSb array. Absorbance (OD = optical density) is calculated on every shot as $-\log(\text{signal/reference})$. For ps resolution, the UV pump is produced by frequency doubling a portion of the amplified R6G dye laser output. To investigate ns and longer time dynamics, the 266 nm harmonic of a Q-switched Nd:YAG laser, electronically synchronized and timed to the IR probe, is employed instead. Typical UV pulse energies are 5 μJ in the ps regime and 30 μJ in the ns studies. The pump is shuttered at 10 Hz and differential absorption spectra calculated by subtracting the un-pumped absorbance spectrum from the pumped absorbance spectrum. We typically averaged 3000 to 4000 laser shots to obtain a single difference spectrum. Several of these spectra were then averaged to obtain the results presented here. Delta (OD) intensity values fall within an uncertainty of ± 0.005 OD units estimated from multiple scan averages (type B, $k = 1$).

For the present study, the Mn complexes were dissolved in *n*-heptane (Mallinckrodt, analytical grade, used as received) at millimolar concentrations to attain $\sim\text{OD } 1$ at the centers of the two CO-stretching absorption bands near 1960 cm^{-1} . During experiments, the heptane solutions were kept at room temperature and circulated through a 1 mm path length cell capped by CaF₂ windows.

Results and Discussion

Irradiation of the bis(methyl sulfide) complex **2** at either 289 or 266 nm leads to rapid reaction. Spectra at early time delays (< 50 ps) are complicated by vibrational cooling dynamics from the initial electronic excitation, but a bleach of the double CO-stretching band at $1953\text{ cm}^{-1}/1964\text{ cm}^{-1}$ is clearly observed, indicating efficient CO extrusion (Figure 1). Transient spectra acquired with probe delays ranging from 100 ps to 1 μs bear the same features evidenced in the corresponding spectra of **1** (which has a single pendant sulfide) after photolysis.⁴ At

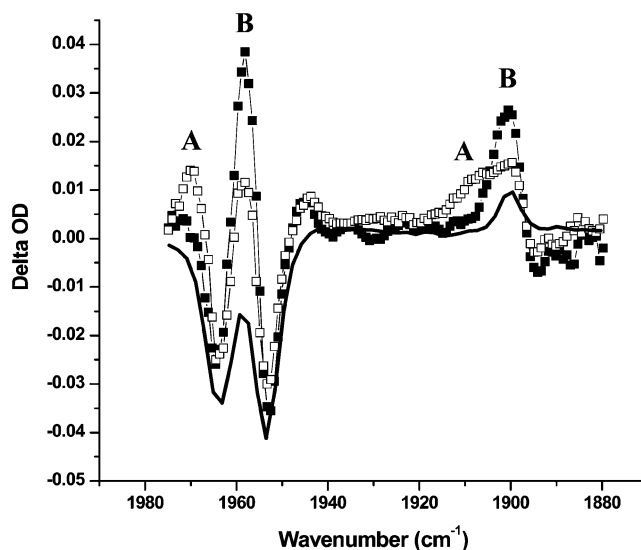


Figure 1. Average of transient spectra (open square curve) acquired 5, 10, and 15 ns after 266 nm photolysis of **2** in *n*-heptane solution (this and all subsequent curves are interpolated with a cubic spline). The closed-square curve is an average of transient spectra of the same solution at 200, 500, and 1000 ns delay times. The solid line curve is a difference of two FTIR spectra of **2** in *n*-heptane solution, acquired before and after irradiation with a Hg lamp. Peaks marked “A” are assigned to the solvate complex, whereas those marked “B” are assigned to the sulfur chelate.

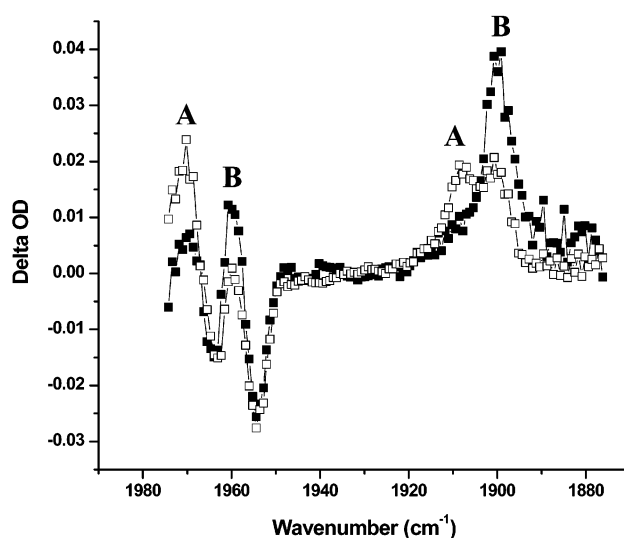


Figure 2. Transient spectrum (open square curve) acquired 10 ns after 266 nm photolysis of **1** in *n*-hexane solution. The closed-square curve is a transient spectrum of the same solution at 110 ns delay time. Peaks marked “A” are assigned to the solvate complex, whereas those marked “B” are assigned to the sulfur chelate.

intermediate time delays (100 ps to 20 ns) there are two pairs of features in the CO-stretching region aside from the parent bleaches: two overlapping bands at 1900 and 1906 cm^{-1} , and two additional bands, somewhat diminished by the bleach feature, at 1958 and 1971 cm^{-1} . At long time delays (> 100 ns), the species responsible for the blue-lying band in each pair (1906 cm^{-1} , 1971 cm^{-1}) has disappeared.

Figure 1 shows two representative transient spectra of **2** at intermediate (open squares) and long (closed squares) time delays. For comparison, analogous spectra from our earlier studies of **1** (bearing one pendant sulfide) are reproduced in Figure 2. In our previous report, we assigned the blue-lying bands in each pair (marked A in the figures) to an alkane solvate of the unsaturated Mn dicarbonyl complex, based in part on

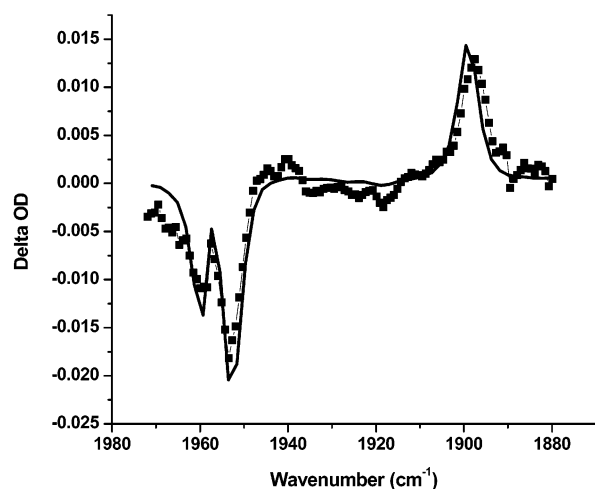


Figure 3. Average of transient spectra (closed square curve) acquired for a 20–100 ps delay time range after 289 nm photolysis of **3** in *n*-heptane solution. The solid line curve is a difference of two FTIR spectra of **3** in *n*-heptane solution, acquired before and after irradiation with a Hg lamp.

studies of $[\eta^5\text{-C}_5\text{H}_4\text{C}(\text{O})\text{CH}_3]\text{Mn}(\text{CO})_3$.⁴ The lower frequency bands in each pair (marked B) are assigned to the chelated product, with the sulfide coordinated to Mn. This product is stable and fully characterized.⁴ In studies of **1**, the bands near 1900 cm^{-1} were sufficiently well-resolved to measure the time constant for conversion of the solvate to the S-chelated species. Unfortunately, the bands in the present study of **2** are too poorly resolved to permit detailed kinetic measurements. It is nonetheless clear from comparison of Figures 1 and 2 that the photoinduced dynamics of compounds **1** and **2** do not differ appreciably.

We also show in Figure 1 a differential FTIR spectrum of **2** obtained after UV lamp irradiation of a solution of this species in *n*-heptane. The FTIR spectrum has been scaled to match the bleach intensity of the transient spectra, and the decrease in the relative intensity of the product band suggests that the chelated photoproduct is somewhat unstable and may decompose upon extended irradiation.

Figure 3 reveals the photochemical behavior of tris(methyl sulfide) complex **3** (closed squares). The curve plotted with closed squares is an average of transient spectra acquired in the 20–100 ps range following 289 nm photolysis of **3** in heptane solution. For comparison, this trace is overlaid with a static difference spectrum, acquired by FTIR after prolonged UV lamp irradiation of a solution of **3** and scaled to the bleach intensity of the transient spectrum. In stark contrast to the behavior exhibited by complexes **1** and **2**, there is no evidence in the transient spectrum of **3** for a solvated species. Only features assigned to the S-chelated product appear in the spectrum. No significant changes in the spectrum were observed

at later time delays. As Figure 3 clearly shows, there is excellent agreement between the features in the transient trace and those in the FTIR difference spectrum of the stable product. We conclude, therefore, that 100 ps is an upper bound on the time scale for complete formation of the chelate product stemming from photolysis of **3**. Due to signal-to-noise limitations (± 0.005 OD), we cannot conclusively rule out some degree of solvate formation at very early times, though we consider this possibility unlikely. We can, however, state definitively that any solvate formed on photolysis of **3** is transformed to the chelate at a rate 3 orders of magnitude greater than that of the analogous transformations observed on photolysis of **1** and **2**. Additionally, comparison of the FTIR spectra in Figures 1 and 3 suggests that the chelate formed from **3** is more stable to extended photolysis than the analogue derived from **2**.

It remains unclear why addition of a second pendant sulfide has no impact on the chelation dynamics, while the presence of a third so effectively restricts competing solvation. The results suggest a strong conformational bias for the sulfide groups to point away from the metal center if hydrogen is present as an alternative. Previously, we used molecular modeling to show that **1** had essentially two stable conformations: either the sulfide was above the Cp plane and away from the metal or below the Cp plane and close to the metal, effectively excluding solvent between the sulfur and the metal.⁴ We postulated that upon CO dissociation the former conformation led immediately to solvate and the latter to chelate. In the current study, conformational energies of **2** were determined by MM3 calculations. The dihedral angle for atoms 3–6–7–8 (Figure 4) was locked at 0° while the energies were minimized in 15° dihedral angle increments for atoms 1–2–3–4 and 2–3–4–5 and in 30° dihedral angle increments for atoms 4–3–6–7. From these 6912 conformations, the minimum energy conformation was obtained for every 4–3–6–7 dihedral angle increment. The remaining angle restrictions were lifted on these 12 conformations and after further energy minimization only six conformations were unique. Five of these were of similar energy and had 4–3–6–7 dihedral angles of $+61^\circ$, -81° , and -160° with relative energies of 0.7, 0.7, and 0.0 kcal mol^{-1} , respectively (Figure 4; the two additional conformations not shown in Figure 4 have 4–3–6–7 dihedral angles of 61° , but the methyl groups were rotated about 120° into other energy equivalent positions). Unlike the other conformations, the lowest energy conformation (-160° 4–3–6–7 dihedral angle) does not have the sulfur adjacent to the metal and will not lead to ultrafast chelation. In stark contrast, examination of the analogous potential landscape reveals that all low energy conformations of **3** have a sulfide near the metal, allowing chelation to occur on every CO dissociation.

We note, finally, that CO extrusion should sometimes occur on the opposite side of the complex from the acyl moiety, ostensibly affording easy access to a solvent molecule irrespec-

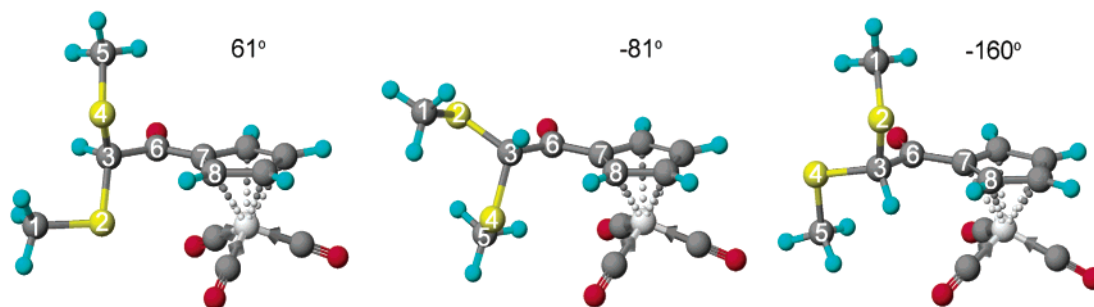


Figure 4. Minimum energy conformations of **2** with S(4)–C(3)–C(6)–C(7) dihedral angles of $+61^\circ$, -81° , and -160° .

tive of the number of pendant sulfides. One explanation for the apparent lack of a solvation pathway after photolysis of **3** may be that Cp-ring in-plane rotation occurs more rapidly than CO diffusion out of the solvent cage. Alternatively, rapid rehybridization at the metal center may permit backside sulfur coordination relative to the departing CO. Molecular dynamics and related modeling are clearly required to better understand the structural dynamics of these systems.

Summary

We have investigated the UV photoinduced dynamics of complexes **2** and **3**, which bear two and three pendant methyl sulfide groups, respectively, poised near a photoreactive Mn(CO)₃ center. Both complexes exhibit efficient CO loss. Compound **2**, in direct analogy to the previously studied Mn species **1** (bearing only a single sulfide group), is subject after CO dissociation to a competition between sulfide and solvent for coordination of the unsaturated Mn. Initially, the product distribution is approximately evenly divided between ring-closed and solvated species; as was observed with **1**, the solvate is converted to the more stable ring-closed product within 200 ns. Compound **3**, with three pendant sulfide groups, shows no

evidence for competitive formation of solvate upon photolytic CO loss. The formation of the photostable chelate species derived from **3** is complete within 100 ps after UV excitation. These results suggest that chelation without extensive conformational changes can exclude ultrafast processes such as solvation.

References and Notes

- (1) (a) Snee, P. T.; Payne, C. K.; Kotz, K. T.; Yang, H.; Harris, C. B. *J. Am. Chem. Soc.* **2001**, *123*, 2255–2264. (b) Yang, H.; Asplund, M. C.; Kotz, K. T.; Wilkens, M. J.; Frei, H.; Harris, C. B. *J. Am. Chem. Soc.* **1998**, *120*, 10154–10165.
- (2) Giordano, P. J.; Wrighton, M. S. *Inorg. Chem.* **1977**, *16*, 160–166.
- (3) (a) Kim, S. K.; Pedersen, S.; Zewail, A. H. *Chem. Phys. Lett.* **1995**, *233*, 500. (b) Schwartz, B. J.; King, J. C.; Zhang, J. Z.; Harris, C. B. *Chem. Phys. Lett.* **1993**, *203*, 503–508. (c) Winnik, M. A. *Chem. Rev.* **1981**, *81*, 491–524.
- (4) Jiao, T.; Pang, Z.; Burkey, T. J.; Johnston, R. F.; Heimer, T. A.; Kleiman, V. D.; Heilweil, E. J. *J. Am. Chem. Soc.* **1999**, *121*, 4618–4624.
- (5) Barbero, M.; Cadamuro, S.; Degani, I.; Dughera, S.; Fochi, R. *J. Org. Chem.* **1995**, *60*, 6017–6024.
- (6) ¹H NMR (CDCl₃): **2**, δ 2.12 (s, 6H, –SCH₃), 4.59 (s, 1H, CH), 4.86 (t, 2H, *J* 2.2, C₅H₄^{3,4}), 5.51 (t, 2H, *J* 2.2, C₅H₄^{2,5}); **3**, δ 2.07 (s, 9H, –SCH₃), 4.80 (m, 2H, C₅H₄^{3,4}), 5.90 (m, 2H, C₅H₄^{2,5}).